*Inorg. Chem.* **2007**, *46*, 7494–7502


# Effect of Axial Coordination on the Electronic Structure and Biological Activity of Dirhodium(II,II) Complexes

**J. Dafhne Aguirre,[†] Daniel A. Lutterman,[‡] Alfredo M. Angeles-Boza,[†] Kim R. Dunbar,*[,†] and Claudia Turro*[,‡]**

*Department of Chemistry, The Ohio State University, Columbus, Ohio 43210, and Department of Chemistry, Texas A&M University, College Station, Texas 77843*

Received April 13, 2007

The reactivities toward biomolecules of a series of three dirhodium(II,II) complexes that possess an increasing number of accessible axial coordination sites are compared. In *cis*-$[Rh_2(OAc)_2(np)_2]^{2+}$ (**1**; np = 1,8-naphthyridine) both axial sites are available for coordination, whereas for *cis*-$[Rh_2(OAc)_2(np)(pynp)]^{2+}$ (**2**; pynp = 2-(2-pyridyl)1,8-naphthyridine) and *cis*-$[Rh_2(OAc)_2(pynp)_2]^{2+}$ (**3**) the bridging pynp ligand blocks one and two of the axial coordination sites in the complexes, respectively. The electronic absorption spectra of the complexes are consistent with strong metal-to-ligand charge transfer transitions at low energy and ligand-centered peaks localized on the np and/or pynp ligands in the UV and near-UV regions. Time-dependent density functional theory calculations were used to aid in the assignments. The three complexes exhibit metal-centered oxidations and reductions, localized on the aromatic ligands. The ability of the complexes to stabilize duplex DNA and to inhibit transcription *in vitro* is greatly affected by the availability of an open axial coordination site. The present work shows that open axial coordination sites on the dirhodium complexes are necessary for biological activity.

## Introduction

The principal mode of action of many antitumor drugs and antiviral agents takes place through the disruption of transcription and related processes.[1−4] These include anticancer agents such as actinomycin D,[5−7] anthracycline antibiotics,[8,9] daunorubicin,[10,11] and cisplatin,[12,13] among others.[14−23] In general, the inhibition of transcription by these drugs takes place through their interaction with, modification of, or damage to template DNA,[5−13] but in some cases the mechanism involves the binding of the drug to the active

* To whom correspondence should be addressed. E-mail: turro@chemistry.ohio-state.edu (C.T.), dunbar@mail.chem.tamu.edu (K.R.D).
[†]Texas A&M University.
[‡]The Ohio State University.

(1) Darnell, J. E., Jr. *Nat. Rev. Cancer* **2002**, *2*, 740.
(2) Zhou, M. *Curr. Cancer Therapy Rev.* **2006**, *2*, 331.
(3) Kim, R.; Tanabe, K.; Emi, M.; Uchida, Y.; Inoue, H.; Toge, T. *Anti−Cancer Drugs* **2003**, *14*, 3.
(4) Popa, C.; Dahler, A. L.; Serewko-Auret, M.; Saunders, N. *Trends Chemother. Res.* **2006**, 25.
(5) Imamichi, T.; Murphy, M. A.; Adelsberger, J. W.; Yang, J.; Watkins, C. M.; Berg, S. C.; B., Michael W.; L., Richard A.; Guo, J.; Levin, J. G.; Lane, H. C. *J. Virol.* **2003**, *77*, 1011.
(6) Chang, T.-C.; Tsai, L.-C.; Hung, M.-W.; Chu, L.-.; Chu, J.-T.; Chen, Y.-C. *Biochem. Pharmacol.* **1997**, *53*, 969.
(7) (a) Blagosklonny, M. V. *Cell Cycle* **2004**, *3*, 1537−1542. (b) Phillips, D. R.; Crothers, D. M. *Biochemistry* **1986**, *25*, 7355.
(8) Mansilla, S.; Rojas, M.; Bataller, M.; Priebe, W.; Portugal, J. *Biochem. Pharmacol.* **2007**, *73*, 934.
(9) (a) Bakker, M.; van der Graaf, W. T. A.; Groen, H. J. M.; Smit, E. F.; De Vries, E. G. E. *Curr. Pharm. Des.* **1995**, *1*, 133. (b) Jiang, X. R.; Macey, M. G.; Kelsey, S. M.; Collins, P. W.; Gutteridge, C. N.; Miki, T.; Adachi, K.; Yamabe, S.; Newland, A. C. *J. Chemother.* **1993**, *5*, 334.
(10) Antoniou, T.; Tseng, A. L. *Clin. Pharmacokinet.* **2005**, *44*, 111.
(11) (a) Portugal, J.; Martin, B.; Vaquero, A.; Ferrer, N.; Villamarin, S.; Priebe, W. *Curr. Med. Chem.* **2001**, *8*, 1. (b) Marin, S.; Mansilla, S.; Garcia-Reyero, N.; Rojas, M.; Portugal, J.; Pina, B. *Biochem. J.* **2002**, *368*, 131.
(12) Jamieson, E. R.; Lippard, S. J. *Chem. Rev.* **1999**, *99*, 2467.
(13) O'Dwyer, P. J.; Stevenson, J. P.; Johnson, S. W. In *Cisplatin: Chemistry and Biochemistry of a Leading Anticancer Drug*; Lippert, B., Ed.; Wiley-VCH: Weinheim, 1999, pp 31−69.
(14) (a) Chu, W.; Shinomya, M.; Kamitori, K. Y.; Kamitori, S.; Carlson, R. G.; Weaver, R. F.; Takusagawa, F. *J. Am. Chem. Soc.* **1994**, *116*, 7971. (b) Takusagawa, F.; Carlson, R. G.; Weaver, R. F. *Bioorg. Med. Chem.* **2001**, *9*, 719.
(15) Kester, H. A.; Blanchetot, C.; Den Hertog, J.; Van der Saag, P. T.; Van der Burg, B. *J. Biol. Chem.* **1999**, *274*, 27439.
(16) Taatjes, D. J.; Gaudiano, G.; Resing, K.; Koch, T. *J. Med. Chem.* **1997**, *40*, 1276.
(17) (a) Cullinane, C.; Mazur, S. J.; Essigmann, J. M.; Phillips, D. R.; Bohr, V. A. *Biochemistry* **1999**, *38*, 6204. (b) Trimmer, E. E.; Essigmann, J. M. *Essays Biochem.* **1999**, *34*, 191.
(18) Aune, G. J.; Furuta, T.; Pommier, Y. *Anti-Cancer Drugs* **2002**, *13*, 545.
(19) Gojo, I.; Zhang, B.; Fenton, R. G. *Clin. Cancer Res.* **2002**, *8*, 3527.
(20) Gillet, R.; Bobichon, H.; Trentesaux, C. *Biol. Cell.* **2002**, *94*, 267.
(21) Jaspers, N. G. J.; Raams, A.; Kelner, M. J.; Ng, J. M. Y.; Yamashita, Y. M.; Takeda, S.; McMorris, T. C.; Hoeijmakers, J. H. J. *DNA Repair* **2002**, *1*, 1027.



10.1021/ic700708g CCC: $37.00 © 2007 American Chemical Society
Published on Web 08/09/2007

site of RNA polymerase, blocking of the DNA/RNA channel,[24,25] or by targeting transcription factors.[26] The developed cellular resistance and the effectiveness of each agent against certain cancers but not others are limitations of the current drugs, which have prompted the search for new compounds.[27−32]

Dirhodium(II) tetracarboxylate complexes, $Rh_2(\mu\text{-}O_2CR)_4$ (R = Me, Et, Pr, Bu), and related compounds exhibit carcinostatic activity against Ehrlich ascites and leukemia L1210 tumors,[33,34] and they have been shown to be antibacterial and antitumor agents.[35] In some cases, the antitumor activity *in vitro* was reported to be of the same order of magnitude as that of the anticancer drug cisplatin.[36] Cisplatin covalently binds to double-stranded DNA (ds-DNA) by forming primarily 1,2-d(GpG) intrastrand cross-links, which disrupt the normal function of proteins and the transcription process.[37−40] Although the mechanism of action of the dirhodium complexes remains largely unknown, it has been established that the complexes inhibit DNA replication and transcription *in vitro*.[41−43] Transcription inhibition by $Rh_2$(II,II) complexes is believed to involve binding of the compound to either template DNA or RNA polymerase and to depend, among other factors, on the ligation sphere around the dirhodium core.[42,43]

Dirhodium complexes have been shown to bind to nucleobases,[44−46] dinucleotides,[47] and DNA dodecamer single strands[48] through both axial and equatorial ligand substitution. It is believed, however, that for complexes where equatorial substitution takes place, the initial interaction is axial followed by shifting of the new axial ligand to an equatorial position.[49,50] Therefore, it is expected that the presence of strong, nonlabile ligands in the axial position of a dirhodium(II,II) complex would decrease the observed bioactivity through decreased interactions or binding of the compounds to biomolecules. In the present work, complexes that possess one or two accessible axial coordination sites are compared to a compound in which the axial positions are blocked. In the case of *cis*-$[Rh_2(OAc)_2(np)_2]^{2+}$ (**1**; np = 1,8-naphthyridine), both axial sites are available for coordination whereas for *cis*-$[Rh_2(OAc)_2(np)(pynp)]^{2+}$ (**2**; pynp = 2-(2-pyridyl)1,8-naphthyridine) and *cis*-$[Rh_2(OAc)_2(pynp)_2]^{2+}$ (**3**), the bridg-


(22) Gajate, C.; An, F.; Mollinedo, F. *J. Biol. Chem.* **2002**, *277*, 41580.
(23) Rokhlin, O. W.; Glover, R. A.; Taghiyev, A. F.; Guseva, N. V.; Seftor, R. E. B.; Shyshynova, I.; Gudkov, A. V.; Cohen, M. B. *J. Biol. Chem.* **2002**, *277*, 33213.
(24) Campbell, E. A.; Korzheva, N.; Mustaev, A.; Murakami, K.; Nair, S.; Goldfarb, A.; Darst, S. A. *Cell* **2001**, *104*, 901.
(25) Luo, G.; Lewis, R. A. *Biochem. Pharmacol.* **1992**, *44*, 2251.
(26) Chao, S.-H.; Price, D. H. *J. Biol. Chem.* **2001**, *276*, 31793.
(27) Goldie, J. H. *Cancer Metastasis Rev.* **2001**, *20*, 63.
(28) Tolomeo, M.; Simoni, D. *Curr. Med. Chem.: Anti-Cancer Agents* **2002**, *2*, 387.
(29) Broxterman, H. J.; Georgopapadakou, N. *Drug Resist. Updates* **2001**, *4*, 197.
(30) Schoendorf, T.; Neumann, R.; Benz, C.; Becker, M.; Riffelmann, M.; Goehring, U.-J.; Sartorius, J.; von Koenig, C.-H. W.; Breidenbach, M.; Valter, M. M.; Hoopmann, M.; Di Nicolantonio, F.; Kurbacher, C. M. *Recent Res. Cancer Res.* **2003**, *161*, 111.
(31) Kanzaki, A.; Takebayashi, Y.; Ren, X.-Q.; Miyashita, H.; Mori, S.; Akiyama, S.-I.; Pommier, Y. *Mol. Cancer Ther.* **2002**, *1*, 1327.
(32) Papadopoulos, K. P.; Sherman, W. H. *Am. J. Cancer* **2002**, *1*, 323.
(33) (a) Erck, A.; Rainen, L.; Whileyman, J.; Chang, I.; Kimball, A. P.; Bear, J. L. *Proc. Soc. Exp. Biol. Med.* **1974**, *145*, 1278. (b) Bear, J. L.; Gray, H. B.; Rainen, L.; Chang, I. M.; Howard, R.; Serio, G.; Kimball, A. P. *Cancer Chemother. Rep.* Part I **1975**, *59*, 611. (c) Howard, R. A.; Spring, T. G.; Bear, J. L. *Cancer Res.* **1976**, *36*, 4402. (d) Erck, A.; Sherwood, E.; Bear, J. L.; Kimball, A. P. *Cancer Res.* **1976**, *36*, 2204. (e) Howard, R. A.; Sherwood, E.; Erck, A.; Kimball, A. P.; Bear, J. L. *J. Med. Chem.* **1977**, *20*, 943. (f) Bear, J. L.; Howard, R. A.; Dennis, A. M. *Curr. Chemother.* **1978**, 1321. (g) Howard, R. A.; Kimball, A. P.; Bear, J. L. *Cancer Res.* **1979**, *39*, 2568. (h) Rao, P. N.; Smith, M. L.; Pathak, S.; Howard, R. A.; Bear, J. L. *J. Natl. Cancer Inst.* **1980**, *64*, 905. (i) Bear, J. L. In *Precious Metals 1985: Proceedings of the Ninth International Precious Metals Conference*; Zysk, E. E., Bonucci, J. A., Eds.; Int. Precious Metals: Allentown, PA, 1986; pp 337−344.
(34) (a) Esposito, B. P.; Faljoni-Alário, A.; Silva, de Menezes, J. F.; Felinto de Brito, H.; Najjar, R. *J. Inorg. Biochem.* **1999**, *75*, 55. (b) Esposito, B. P.; Zyngier, S. B.; Najjar, R.; Paes, R. P.; Ueda, S. M. Y.; Barros, J. C. A. *Met. Based Drugs* **1999**, *1*, 17. (c) Esposito, B. P.; de Oliviera, E.; Zygnier, S. B.; Najjar, R. *J. Braz. Chem. Soc.* **2000**, *11*, 447. (d) Esposito, B. P.; Najjar, R. *Coord. Chem. Rev.* **2002**, *232*, 137.
(35) (a) Bien, M.; Pruchnik, F. P.; Seniuk, A.; Lachowicz, T. M.; Jakimowicz, P. *J. Inorg. Biochem.* **1999**, *73*, 49. (b) Pruchnik, F. P.; Starosta, R.; Ciunik, Z.; Opolski, A.; Wietrzyk, J.; Wojdat, E.; Dus, D. *Can. J. Chem.* **2001**, *79*, 868. (c) Pruchnik, F. P.; Jakimowicz, P.; Ciunik, Z.; Zakrzewska-Czerwinska, J.; Opolski, A.; Wietrzyk, J.; Wojdat, E. *Inorg. Chim. Acta* **2002**, *334*, 59. (d) Pruchnik, F. P.; Banbula, M.; Ciunik, Z.; Chojnacki, H.; Latocha, M.; Skop, B.; Wilczok, T.; Opolski, A.; Wietrzyk, J.; Nasulewicz, A. *Eur. J. Inog. Chem.* **2002**, 3214. (e) Pruchnik, F. P.; Banbula, M.; Ciunik, Z.; Chojnacki, H.; Latocha, M.; Skop, B.; Wilczok, T. *Appl. Organomet. Chem.* **2002**, *16*, 587.
(36) (a) Reibscheid, E. M.; Zyngier, S.; Maria, D. A.; Mistrone, R. J.; Sinisterra, R. D.; Couto, L. G.; Najjar, R. *Braz. J. Med. Biol. Res.* **1994**, *27*, 91. (b) Esposito, B. P.; Zyngier, S. B.; Ribeiro de Souza, A.; Najjar, R. *Met. Based Drugs*, **1997**, *4*, 333.
(37) (a) Yarnell, A. T.; Oh, S.; Reinberg, D.; Lippard, S. J. *J. Biol. Chem.* **2001**, *276*, 25736. (b) Cohen, S. M.; Jamieson, E. R.; Lippard, S. J. *Biochemistry* **2000**, *39*, 8259. (c) Zamble, D. B.; Lippard, S. J. In *Cisplatin: Chemistry and Biochemistry of a Leading Anticancer Drug*; Lippert, B., Ed.; Wiley-VCH: Weinheim, 1999; pp 73−110.
(38) (a) Wozniak, K.; Blasiak, J. *Acta Biochim. Pol.* **2002**, *49*, 583. (b) Wozniak, K.; Walter, Z. *Cell Biol. Int.* **2002**, *26*, 495.
(39) Fuertes, M. A.; Castilla, J.; Alonso, C.; Perez, J. M. *Curr. Med. Chem.* **2003**, *10*, 257.
(40) (a) Zamble, D. B.; Mikata, Y.; Eng, C. H.; Sandman, K. E.; Lippard, S. J. *J. Inorg. Biochem.* **2002**, *91*, 451. (b) Trimmer, E. E.; Zamble, D. B.; Lippard, S. J.; Essigmann, J. M. *Biochemistry* **1998**, *37*, 352. (c) McA'Nulty, M. M.; Whitehead, J. P.; Lippard, S. J. *Biochemistry* **1996**, *35*, 6089. (d) Huang, J.-C.; Zamble, D. B.; Reardon, J. T.; Lippard, S. J.; Sancar, A. *Proc. Natl. Acad. Sci. U.S.A.* **1994**, *91*, 10394.
(41) Dale, L. D.; Dyson, T. M.; Tocher, D. A.; Tocher, J. H.; Edwards, D. I. *Anti-Cancer Drug Des.* **1989**, *4*, 295.
(42) Sorasaenee, K.; Fu, P. K.-L.; Angeles-Boza, A. M.; Dunbar, K. R.; Turro, C. *Inorg. Chem.* **2003**, *42*, 1267.
(43) (a) Chifotides, H. T.; Fu, P. K.-L.; Dunbar, K. R.; Turro, C. *Inorg. Chem.* **2004**, *43*, 1175. (b) Angeles-Boza, A. M.; Chifotides, H. T.; Aguirre, J. D.; Chouai, A.; Fu, P. K.-L.; Dunbar, K. R.; Turro, C. *J. Med. Chem.* **2006**, *49*, 6841.
(44) (a) Dunbar, K. R.; Matonic, J. H.; Saharan, V. P.; Crawford, C. A.; Christou, G. *J. Am. Chem. Soc.* **1994**, *116*, 2201. (b) Day, E. F.; Crawford, C. A.; Folting, K.; Dunbar, K. R.; Christou, G. *J. Am. Chem. Soc.* **1994**, *116*, 9339. (c) Crawford, C. A.; Day, E. F.; Saharan, V. P.; Folting, K.; Huffman, J. C.; Dunbar, K. R.; Christou, G. *Chem. Commun.* **1996**, 1113. (d) Catalan, K. V.; Mindiola, D. J.; Ward, D. L.; Dunbar, K. R. *Inorg. Chem.* **1997**, *36*, 2458. (e) Catalan, K. V.; Hess, J. S.; Maloney, M. M.; Mindiola, D. J.; Ward, D. L.; Dunbar, K. R. *Inorg. Chem.* **1999**, *38*, 3904.
(45) Rubin, J. R.; Haromy, T. P.; Sundaralingam, M. *Acta Crystallogr.* **1991**, *C47*, 1712.
(46) Aoki, K.; Salam, M. A. *Inorg. Chim. Acta*, **2001**, *316*, 50.
(47) Chifotides, H. T.; Koshlap, K. M.; Pérez, L. M.; Thomson, L. M.; Dunbar, K. R. *J. Am. Chem. Soc.* **2003**, *125*, 10703.
(48) Asara, J. M.; Hess, J. S.; Lozada, E.; Dunbar, K. R.; Allison, J. *J. Am. Chem. Soc.* **2000**, *122*, 8.
(49) (a) Perlepes, S. P.; Huffman, J. C.; Matonic, J. H.; Dunbar, K. R.; Christou, G. *J. Am. Chem. Soc.* **1991**, *113*, 2770. (b) Crawford, C. C.; Matonic, J. H.; Streib, W. E.; Huffman, J. C.; Dunbar, K. R.; Christou, G. *Inorg. Chem.* **1993**, *32*, 3125.
(50) Rotondo, E.; Mann, B. E.; Piraino, P.; Tresoldi, G. *Inorg. Chem.* **1989**, *28*, 3070.

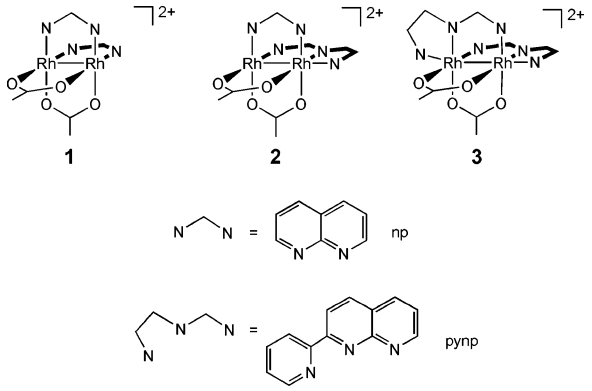


**Figure 1.** Schematic representation of the molecular structures of **1**−**3** and the np and pynp ligands.

ing pynp ligand blocks one and two of the axial coordination sites in the complexes, respectively. The structures of **1**−**3** are shown in Figure 1. The electronic and electrochemical properties of the complexes were investigated and density functional theory (DFT) and time-dependent DFT (TDDFT) calculations were used to aid in the assignments. The ability of the complexes to inhibit transcription *in vitro* shows a profound effect on the availability of an axial coordination site indicating the need of metal binding for biological activity in these complexes.

## Experimental Section

**Materials.** Biotech grade acetonitrile was purchased from Sigma-Aldrich, while tetra-*n*-butylammonium hexafluorophosphate ($TBAPF_6$) was purchased from Fluka. Agarose, ethidium bromide, EDTA, Tris/HCl, $MgCl_2$, and RNA loading solution were purchased from Sigma and used as received. The pGEM linear DNA control template (3995 bp) was purchased from Promega, and the T7−RNA polymerase (50 units/$\mu$L) and 5× RNA transcription buffer were purchased from Life Technologies (Rockville, MD). Calf-thymus DNA was purchased from Sigma and was dialyzed against 5 mM Tris, 50 mM NaCl, pH = 7.5, three times during a 48 h period prior to use. Sonicated herring sperm DNA was purchased from Invitrogen and used as received. $RhCl_3 \cdot xH_2O$ was purchased from Pressure Chemicals, and the starting materials $Rh_2(\mu\text{-}O_2CCH_3)_4$ and *cis*-$[Rh_2(\mu\text{-}O_2CCH_3)_2(CH_3CN)_6](BF_4)_2$ were prepared following literature procedures.[51] The bridging ligand np was purchased from TCI (Tokyo, Japan), while pynp was prepared according to literature procedures.[52] The compounds *cis*-$[Rh_2(\mu\text{-}O_2CCH_3)_2(pynp)_2]^{2+}$ and *cis*-$[Rh_2(\mu\text{-}O_2CCH_3)_2(np)_2]^{2+}$ were synthesized from *cis*-$[Rh_2(\mu\text{-}O_2CCH_3)_2(CH_3CN)_6]^{2+}$ using a modified literature procedure described in detail below.[52]

***cis*-$[Rh_2(\mu\text{-}O_2CCH_3)_2(np)_2](BF_4)_2$.** The tetrafluoroborate salt of *cis*-$[Rh_2(\mu\text{-}O_2CCH_3)_2(CH_3CN)_6]^{2+}$ (0.1 g, 0.13 mmol) was dissolved in acetonitrile (20 mL) to afford a purple solution, to which 2 equiv of the np ligand (0.034 g, 0.26 mmol) was added. The mixture was refluxed and stirred overnight, the solution was evaporated, and a dark-red powder was obtained by filtration. The product was then dissolved in a minimum amount of acetonitrile and toluene was added to precipitate the red-orange product, which was then collected and dried (0.074 g, 74%). $^1$H NMR in $CH_3CN$-$d_6$, $\delta$/ppm: 9.05 (q, 4H), 8.37 (d, 4H), 7.61 (m, 4H), 2.40 (s, 6H). Anal. Calcd for $Rh_2C_{20}H_{18}N_4O_4B_2F_8$: C, 31.70; H, 2.39; N, 7.39. Found: C, 31.65; H, 2.53; N, 7.43.

***cis*-$[Rh_2(\mu\text{-}O_2CCH_3)_2(pynp)_2](BF_4)_2$.** A procedure similar to that for the synthesis of $[Rh_2(\mu\text{-}O_2CCH_3)_2(np)_2]^{2+}$ was used, with the addition of 2 equiv (0.056 g, 0.27 mmol) of pynp ligand to *cis*-$[Rh_2(\mu\text{-}O_2CCH_3)_2(CH_3CN)_6]^{2+}$ (0.1 g, 0.13 mmol) in acetonitrile (20 mL) to obtain a dark-red solid (0.084 g, 84%). $^1$H NMR in $CH_3CN$-$d_6$, $\delta$/ppm (splitting): 9.70 (d, 2H), 8.87 (m, 4H), 8.70 (d, 2H) 8.67 (m, 4H), 8.50 (dd, 2H), 8.37 (td, 2H), 7.48 (q, 2H), 2.25 (s, 6H). Anal. Calcd for $Rh_2C_{30}H_{24}N_6O_4B_2F_8$: C, 39.51; H, 2.65; N, 9.22. Found: C, 39.54; H, 2.74; N, 9.20.

***cis*-$[Rh_2(\mu\text{-}O_2CCH_3)_2(pynp)(np)](BF_4)_2$.** A solution of $Rh_2(\mu\text{-}O_2CCH_3)_4$ (0.2 g, 0.39 mmol) was stirred overnight in acetone (20 mL) in the presence of 1 equiv of pynp (0.08 g, 0.39 mmol). The product precipitated in the reaction mixture and was collected by filtration. The solid was suspended in methanol (40 mL) and stirred at room temperature until it went into solution. To this solution was added 4 equiv of $NaBF_4$ (0.16 g, 1.44 mmol) and 1 equiv of np (0.05 g, 0.38 mmol). The mixture was stirred overnight, the volume of the solution was decreased to ~6 mL, and filtered using a fine frit. The red-orange solution was treated with toluene to afford a red-orange powder (0.06 g, 30%). $^1$H NMR in $CH_3CN$-$d_6$, $\delta$/ppm (splitting): 10.04 (d, 1H), 9.81 (d, 1H), 9.71 (d, 1H), 9.02 (d, 1H), 8.87 (m, 2H), 8.71 (d, 1H), 8.64 (m, 2H), 8.52 (m, 2H), 8.33 (dd, 1H), 8.15 (dd, 1H), 7.87 (dd, 1H), 7.56 (dd, 1H), 2.21 (s, 6H), 1.82 (s, 6H). MS *m*/*z*: 330.5, $[Rh_2(\mu\text{-}O_2CCH_3)_2(pynp)(np)]^{2+}$. Anal. Calcd for $Rh_2C_{25}H_{21}N_5O_4B_2F_8$: C, 35.97; H, 2.54; N, 8.39. Found: C, 35.93; H, 2.39; N, 8.41.

**Instrumentation.** X-ray diffraction data were collected on a Bruker SMART 1000 CCD diffractometer with graphite monochromated Mo K$\alpha$ radiation ($\lambda$ = 0.71073 Å). The frames were integrated with the Bruker SAINT software,[53] and a semiempirical absorption correction using multiple-measured reflections was applied using SADABS.[54] The structures were solved and refined using X-SEED,[55] a graphical interface to SHELX97.[56] Cyclic voltammetric measurements were performed on a HCH electrochemical analyzer, model 620A. Absorption measurements were performed on a Shimadzu UV 1601PC spectrophotometer, a HP 8453 diode array spectrometer, or a Perkin Elmer Lambda 900 spectrometer. Mass spectra were acquired on a PE SCIEX QSTAR Pulsar electrospray ionization mass spectrometer. The ethidium bromide stained agarose gels (1%) were imaged on an AlphaImager 2000 transilluminator (Alpha Innotech Corporation).

**Methods.** For the X-ray crystallographic analysis, a red prismatic crystal of **1** (approximate dimensions: 0.20 × 0.16 × 0.10 mm$^3$) was selected. The crystal was coated with Paratone oil, transferred to a nylon loop, and placed in a cold $N_2$ stream at 110(2) K. An indexing of the preliminary diffraction patterns indicated that the crystal was monoclinic, and selected refinement parameters are listed in Table 1. A total of 24 689 reflections were collected in the range $2.36 \leq \theta \leq 26.37°$. The data collection covered approximately a hemisphere of reciprocal space by a combination of three or four sets of exposures; each set had a different $\phi$ angle for the crystal, and each exposure covered 0.3° in $\Omega$. The crystal decay, which was monitored by analyzing duplicate reflections, was found to be less than 1%; therefore, no decay correction was applied. During the final cycles of refinement, all atoms with the exception

(51) Pimblett, G.; Garner, C. D.; Clegg, W. *J. Chem. Soc., Dalton Trans.* **1986**, 1257.
(52) Campos-Fernandez, C. S.; Thomson, L. M.; Galan-Mascaros, J. R.; Ouyang, X.; Dunbar, K. R. *Inorg. Chem.* **2002**, *41*, 1523.
(53) *SAINT*, Version 6.34; Bruker AXS Inc.: Madison, WI, 2001.
(54) *SADABS*, Version 2.03; Bruker AXS Inc.: Madison, WI, 2002.
(55) Barbour, L. J. *J. Supramol. Chem.* **2001**, *1*, 189.
(56) Sheldrick, G. M. *SHELX, Programs for Solving and Refining Crystal Structures*; University of Göttingen: Germany, 1997.

**Table 1.** Crystal Data and Structure Refinement for Compound **1**−$(Cl)_2$

| empirical formula | $C_{46}H_{41}BF_4N_8O_8Rh_2$ |
|---|---|
| fw | 719.19 |
| cryst syst | monoclinic |
| space group | $P2_1$ |
| unit cell dimensions | $a = 8.812$ (1) Å<br>$b = 17.293(2)$ Å<br>$c = 17.336(2)$ Å<br>$\alpha = 90°$<br>$\beta = 104.574(2)°$<br>$\gamma = 90°$ |
| vol | 2556.8(5) Å$^3$ |
| $Z$ | 4 |
| density (calculated) | 1.868 Mg/m$^3$ |
| abs coeff | 1.545 mm$^{-1}$ |
| cryst size | 0.20 × 0.16 × 0.10 mm$^3$ |
| reflns | 24689 |
| independent reflns | 5224 [$R_{int} = 0.0395$] |
| GOF on $F^2$ | 1.158 |
| final $R$ indices [I > 2$\sigma$(I)][a] | R1 = 0.0508, wR2 = 0.1193 |
| $R$ indices (all data)[a] | R1 = 0.0604, wR2 = 0.1266 |

[a] $R1 = \Sigma||F_o| - |F_c||/\Sigma|F_o|$; $wR2 = [\Sigma[w(F_o^2 - F_c^2)^2]/\Sigma[w(F_o^2)^2]]^{1/2}$

of hydrogen were refined anisotropically. All hydrogen atoms were placed at calculated positions. The structure was solved and refined in the space group $P2_1/n$. The asymmetric unit contains the cationic *cis*-$[Rh_2(\mu\text{-}O_2CCH_3)_2(np)_2]^{2+}$ molecule with two chloride ions coordinated to the axial positions and with two methanol solvent molecules of crystallization. The final refinement cycle was based on 5224 unique reflections (4302 with $F_o^2 > 2\sigma(F_o^2)$), 327 parameters, and no restraints (R1 = 0.0508, wR2 = 0.1193). The maximum and minimum peaks in the final difference Fourier map corresponded to 3.27 and −0.89 e/Å$^3$, respectively, with a goodness-of-fit value of 1.158.

Electrochemical studies were performed in $CH_3CN$ with 0.1 M $TBAPF_6$ as the supporting electrolyte, a BAS Pt disk as the working electrode (surface area 100 $\mu$m), a Ag/AgCl reference electrode, and a Pt wire as the auxiliary electrode. Ferrocene was used as an internal reference, and under the same experimental conditions the ferrocene/ferrocenium couple was observed at $E_{1/2} = +0.52$ V versus Ag/AgCl electrode.[57] The reduction and oxidation potentials were converted to SCE by subtraction of 0.45 V.[58]

The molecular and electronic structure calculations were performed with DFT using the Gaussian03 (G03) program package.[59] The B3LYP[60−62] functional along with the 6-31G* basis set was used for H, C, N, and O,[63] along with the Stuttgart−Dresden (SDD) energy-consistent pseudopotentials for Rh.[64] Formate ligands were used instead of acetates in the computationally modeled complexes. This procedure has been found to be acceptable in other reported computational studies.[65] All geometries were fully optimized under the conditions of the respective programs. Orbital analysis was completed with Molekel 4.3.[66] Vertical electronic transitions were calculated using TDDFT methods implemented within G03.

The concentration of DNA stock solutions was determined from its absorbance at 260 nm ($\epsilon = 10\,000$ M$^{-1}$ cm$^{-1}$).[67] The methods used to determine the DNA binding constants, $K_b$, of the compounds and the DNA melting temperature have been previously reported, and the errors in the value of $K_b$ typically range from 3 to 7% from the fits and multiple measurements.[67−71] The melting temperature experiments were carried out by monitoring the absorption change at 260 nm while varying the temperature from 25 to 95 °C of a mixture containing 20 $\mu$M complex and 100 $\mu$M calf-thymus DNA (ct-DNA) in 1 mM phosphate buffer, 2 mM NaCl, pH 7.2. The binding constant, $K_b$, was determined by optically titrating 5 $\mu$M metal complexes in a 5 mM Tris/HCl, pH 7.2 buffer at room temperature with ct-DNA up to a final concentration of 200 $\mu$M. The dilution of the compound concentration at the end of each titration was negligible. The $K_b$ values were calculated from fits of the absorption changes as a function of [DNA] as previously described in detail.[72] The relative changes in viscosity were measured on a Cannon-Manning semimicroviscometer. The viscometer was immersed in a constant-temperature water bath (25 °C) controlled by a Neslab (model RTE-100) circulator.

The transcription assay has been previously reported.[38,67,73] In the *in vitro* transcription experiment, the pGEM linear DNA template (120 $\mu$M bases) was used with T7−RNAP, resulting in two transcripts of length 1065 and 2346 bases, and each trial was conducted three times. The transcription reaction was conducted for 45 min at 37 °C (40 mM Tris/HCl, pH = 8.0) in nuclease-free water in the presence of 1.25 units of T7−RNAP, 25 mM NaCl, and 1.0 mM of each ATP, CTP, GTP, and UTP. The inhibition of mRNA production by the dirhodium complexes was detected *in vitro* by the measurement of the mRNA generated upon addition of increasing amounts of metal complex to the assay. The concentration of each complex at which 50% of the RNA is transcribed, $C_{inh}$[50], was calculated by interpolation of the integrated areas of the imaged mRNA signal of each lane of the gel conducted with various concentrations of a given complex. Modifications of these methods were utilized in the various control assays, including those designed to determine the role of binding of the complexes


(57) Gagne, R. R.; Koval, C. A.; Lisensky, G. C. *Inorg. Chem.* **1980**, *19*, 2854.

(58) *Electrochemistry for Chemists*, 2nd ed.; Sawyer, D. T., Sobkowiak, A., Roberts, J. L., Jr., Eds.; Wiley: New York, 1995.

(59) Frisch, M. J.; Trucks, G. W.; Schlegel, H. B.; Scuseria, G. E.; Robb, M. A.; Cheeseman, J. R.; Montgomery, J. A., Jr.; Vreven, T.; Kudin, K. N.; Burant, J. C.; Millam, J. M.; Iyengar, S. S.; Tomasi, J.; Barone, V.; Mennucci, B.; Cossi, M.; Scalmani, G.; Rega, N.; Petersson, G. A.; Nakatsuji, H.; Hada, M.; Ehara, M.; Toyota, K.; Fukuda, R.; Hasegawa, J.; Ishida, M.; Nakajima, T.; Honda, Y.; Kitao, O.; Nakai, H.; Klene, M.; Li, X.; Knox, J. E.; Hratchian, H. P.; Cross, J. B.; Adamo, C.; Jaramillo, J.; Gomperts, R.; Stratmann, R. E.; Yazyev, O.; Austin, A. J.; Cammi, R.; Pomelli, C.; Ochterski, J. W.; Ayala, P. Y.; Morokuma, K.; Voth, G. A.; Salvador, P.; Dannenberg, J. J.; Zakrzewski, V. G.; Dapprich, S.; Daniels, A. D.; Strain, M. C.; Farkas, O.; Malick, D. K.; Rabuck, A. D.; Raghavachari, K.; Foresman, J. B.; Ortiz, J. V.; Cui, Q.; Baboul, A. G.; Clifford, S.; Cioslowski, J.; Stefanov, B. B.; Liu, G.; Liashenko, A.; Piskorz, P.; Komaromi, I.; Martin, R. L.; Fox, D. J.; Keith, T.; Al-Laham, M. A.; Peng, C. Y.; Nanayakkara, A.; Challacombe, M.; Gill, P. M. W.; Johnson, B.; Chen, W.; Wong, M. W.; Gonzalez, C.; Pople, J. A. *Gaussian 03*, revision C.02; Gaussian, Inc.: Wallingford, CT, 2004.

(60) Becke, A. D. *Phys. Rev. A: Gen. Phys.* **1988**, *38*, 3098.

(61) Becke, A. D. *J. Chem. Phys.* **1993**, *98*, 5648.

(62) Lee, C.; Yang, W.; Parr, R. G. *Phys. Rev. B: Condens. Matter Mater. Phys.* **1988**, *37*, 785.

(63) Hehre, W. J.; Radom, L.; Schleyer, P. v. R.; Pople, J. A. *Ab Initio Molecular Orbital Theory*; John Wiley & Sons: New York, 1986.

(64) Andrae, D.; Haeussermann, U.; Dolg, M.; Stoll, H.; Preuss, H. *Theor. Chim. Acta* **1990**, *77*, 123.

(65) Bursten, B. E.; Cotton, F. A. *Inorg. Chem.* **1981**, *20*, 3042.

(66) Flukiger, P. Development of Molecular Graphics Package *MOLEKEL*. Ph.D. Thesis, University of Geneva, Geneva, Switzerland, 1992.

(67) (a) Fu, P. K.-L.; Bradley, P. M.; Turro, C. *Inorg. Chem.* **2003**, *42*, 878. (b) Fu, P. K.-L.; Bradley, P. M.; Turro, C. *Inorg. Chem.* **2003**, *42*, 878.

(68) Nair, R. B.; Teng, E. S.; Kirkland, S. L.; Murphy, C. J. *Inorg. Chem.* **1998**, *37*, 139.

(69) Pyle, A. M.; Rehman, J. P.; Mehoyrer, R.; Kumar, C. V.; Turro, N. J. *J. Am. Chem. Soc.* **1989**, *111*, 3051.

(70) Carter, M. T.; Rodriguez, M.; Bard, A. J. *J. Am. Chem. Soc.* **1989**, *111*, 8901.

(71) Kalsbeck, W. A.; Thorp, H. H. *J. Am. Chem. Soc.* **1993**, *115*, 7146.

(72) Chouai, A.; Wicke, S. E.; Turro, C.; Bacsa, J.; Dunbar, K. R.; Want, D.; Thummel, R. P. *Inorg. Chem.* **2005**, *44*, 5996.

(73) Fu, P. K.-L.; Turro, C. *Chem. Commun.* **2001**, 279.

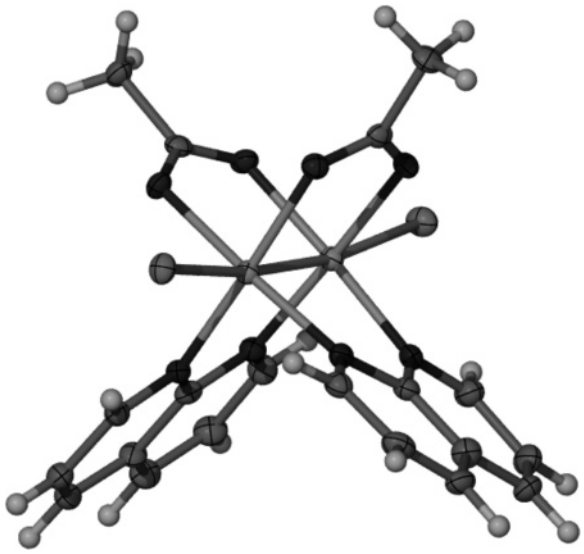

**Figure 2.** Thermal ellipsoid plot at the 50% probability level of **1**−$(Cl)_2$.

to T7−RNAP. All stock solutions of the metal complexes were prepared in pure $H_2O$.

## Results and Discussion

**Synthesis and Characterization.** The bisheteroleptic complexes were prepared by substitution of the four equatorial $CH_3CN$ ligands in *cis*-$[Rh_2(\mu\text{-}O_2CCH_3)_2(CH_3CN)_6]^{2+}$ with the bidentate ligands, np (1,8-naphthyridine) and pynp (2-(2-pyridyl)1,8-naphthyridine), to generate *cis*-$[Rh_2(\mu\text{-}O_2CCH_3)_2(np)_2]^{2+}$ (**1**) and *cis*-$[Rh_2(\mu\text{-}O_2CCH_3)_2(pynp)_2]^{2+}$ (**3**), respectively. The synthesis of the new tris-heteroleptic complex *cis*-$[Rh_2(\mu\text{-}O_2CCH_3)_2(np)(pynp)]^{2+}$ (**2**) was carried out by stepwise addition of pynp followed by np to an acetone solution of $Rh_2(\mu\text{-}O_2CCH_3)_4$ at room temperature. The crystal structure of the dichloride adduct of **1**, which has not been previously reported, is shown in Figure 2.

The molecular structure of **1**, determined by X-ray crystallographic methods, consists of a dinuclear $Rh_2$(II,II) core with a pair of bridging np ligands coordinated to each Rh atom and two bridging acetate groups occupying the remaining equatorial sites. Two chloride ions complete a distorted octahedral coordination sphere around each Rh atom. The structure of **1** is shown in Figure 2 and is similar to those reported for related dirhodium complexes.[52,74,75] A selection of bond distances and angles is listed in Table 2. The Rh−Rh distance in **1**, 2.4251(5) Å, is well within the expected range for a Rh−Rh single bond. The distance is longer than that reported for $[Rh_2(\mu\text{-}O_2CCH_3)_2(pynp)_2]^{2+}$, 2.206(9) Å, and shorter than those reported for $Rh_2(\mu\text{-}O_2CCH_3)_2(phen)_2Cl_2$ (phen = 1,10-phenanthroline) and $[Rh_2(np)_4(O_2CCH_3)_2]^{2+}$, 2.6011(11) and 2.448(1) Å, respectively. The average Rh−N bond length in **1**, 2.027(4) Å, is similar to that of $[Rh_2(\mu\text{-}O_2CCH_3)_2(pynp)_2]^{2+}$, 2.018(4) Å, and longer than the reported Rh−$N_{av}$ distance of 2.010(5) Å in $Rh_2(\mu\text{-}O_2CCH_3)_2(phen)_2Cl_2$ and somewhat shorter than that found for $[Rh_2(np)_4(O_2CCH_3)_2]^{2+}$, 2.054(3) Å. The axial chloride ligands are at an average distance of 2.563(1) Å in **1** whereas the reported Rh−Cl distance for $Rh_2(\mu\text{-}O_2CCH_3)_2(phen)_2Cl_2$ is 2.532(2) Å. This increase of 0.03 Å, as compared to the bis-phenanthroline analogue, can be attributed primarily to the presence of the hydrogen atoms on the np ligands pointing toward the chloride ions.

**Table 2.** Selected Bond Lengths (Å) and Angles (deg) for Compound **1**−$(Cl)_2$

| | | | |
|---|---|---|---|
| Rh1−Rh2 | 2.4251(5) | Rh2−Rh1−Cl1 | 173.46(3) |
| Rh1−N1 | 2.025(4) | Rh1−Rh2−Cl2 | 171.92(3) |
| Rh1−N3 | 2.028(4) | N1−Rh1−N3 | 92.2(2) |
| Rh2−N4 | 2.022(4) | O3−Rh1−O1 | 87.5(1) |
| Rh2−N2 | 2.031(4) | N4−Rh2−N2 | 88.9(2) |
| Rh1−O3 | 2.043(3) | O4−Rh2−O2 | 89.0(1) |
| Rh1−O1 | 2.046(3) | | |
| Rh2−O4 | 2.058(3) | | |
| Rh2−O2 | 2.063(3) | | |
| Rh1−Cl1 | 2.582(1) | | |
| Rh2−Cl2 | 2.544(1) | | |

**Table 3.** Electronic Absorption and Electrochemical Properties of **1**−**3**

| complex | $\lambda_{abs}$/nm ($\epsilon$/$M^{-1}$ $cm^{-1}$)[a] | $E_{1/2}$/V[b] |
|---|---|---|
| **1** | 268 (16 260), 307 (5980), 315 (5830), 393 (4880) | −0.82 |
| **2** | 266 (21 320), 320 (19 490), 356 (5410), 398 (3380) | −0.63, −1.35 |
| **3** | 316 (31 390), 329 (31 400), 356 (12 790), 465 (3680) | −0.64, −1.03 |

[a] In $CH_3OH/H_2O$ (50:50 v/v). [b] In acetonitrile with 0.1 M $Bu_4NPF_6$ vs SCE.

**Electronic Absorption and Electrochemistry.** The absorption maxima and molar extinction coefficients of complexes **1**−**3** are listed in Table 3. Since the free np ligand exhibits $\pi\pi^*$ transitions at 258, 300, and 309 nm in $CH_3OH/H_2O$ (50:50 v/v), it is likely that the peaks observed in **1** at 268 and 307 nm are centered on the np ligand. Similarly, the free pynp ligand exhibits absorption maxima at 271, 322, and 333 (sh) nm in $CH_3OH/H_2O$ (50:50 v/v), which leads to the assignment of the peaks at 316 and 329 nm in **3** as ligand centered. In the mixed-ligand complex **2**, the peaks observed at 266 and 320 nm are likely due to a superposition of $\pi\pi^*$ transitions of the np and pynp ligands. Additional absorption peaks in the UV and near-UV are observed with maxima at 315 nm ($\epsilon$ = 5830 $M^{-1}$ $cm^{-1}$) in **1** and at 356 nm in both **2** ($\epsilon$ = 5410 $M^{-1}$ $cm^{-1}$) and **3** ($\epsilon$ = 12 790 $M^{-1}$ $cm^{-1}$), which may be attributed to metal-to-ligand charge transfer (MLCT) transitions. The latter may correspond to $Rh_2 \rightarrow$ pynp, which is expected at a lower energy than the corresponding MLCT transition to the np ligand in **1**. Each complex also exhibits an absorption peak in the 393−465 nm region with intensity that ranges from 3380 to 4880 $M^{-1}$ $cm^{-1}$. In the related complex $Rh_2(\mu\text{-}O_2CCH_3)_4$, the transitions observed in water in the visible region are weak (441 nm, $\epsilon$ = 106 $M^{-1}$ $cm^{-1}$ and 585 nm, $\epsilon$ = 241 $M^{-1}$ $cm^{-1}$) and have been previously assigned to Rh−O($\sigma$) $\rightarrow$ $Rh_2(\sigma^*)$ and $Rh_2(\pi^*) \rightarrow Rh_2(\sigma^*)$, respectively.[52,76] Owing to the intensity of the transitions observed in **1**−**3** in the visible region, the transitions can be assigned as arising from MLCT from $Rh_2$ to the np and/or pynp ligand depending on the complex. The position and intensity of these transitions are comparable to those observed in *cis*-

(74) Campos-Fernández, C. S.; Ouyang, X.; Dunbar, K. R. *Inorg. Chem.* **2000**, *39*, 2432.
(75) Pruchnik, F. P.; Jutarska, A.; Ciunik, Z.; Pruchnik, M. *Inorg. Chim. Acta* **2004**, *357*, 3019−3026.
(76) Sowa, T.; Kawamura, T.; Shida, T.; Yonezawa, T. *Inorg. Chem.* **1983**, *22*, 56.

$[Rh_2(\mu\text{-}O_2CCH_3)_2(bpy)_2]^{2+}$ (bpy = 2,2′-bipyridine, $\lambda_{abs}$ = 408 nm, $\epsilon$ = 2920 $M^{-1}$ $cm^{-1}$ in $CH_3CN$) and *cis*-$[Rh_2(\mu\text{-}O_2CCH_3)_2(phen)_2]^{2+}$ (phen = 1,10-phenanthroline, $\lambda_{abs}$ = 408 nm, $\epsilon$ = 3050 $M^{-1}$ $cm^{-1}$ in $CH_3CN$), which also possess aromatic ligands coordinated to the dirhodium core and have been previously assigned as MLCT from the $Rh_2$ to the bpy and phen ligand, respectively.[77]

Additional evidence for the assignment of the lowest energy transition in complexes **1**−**3** as MLCT can be obtained by examining the spectrum of **1** with axially coordinated pyridine (py). The presence of strong $\sigma$-donor axial ligands has been shown to have a profound effect on the electronic structure of dirhodium complexes. For example, in $Rh_2(\mu\text{-}O_2CCH_3)_4$ addition of ligands that bind to the axial positions results in a blue shift of the lowest energy, $Rh_2(\pi^*) \rightarrow Rh_2(\sigma^*)$ metal-centered (MC) transition.[78−80] This shift is due to the interaction of the antisymmetric linear combination of the filled orbitals on the axial ligands with the $Rh_2(\sigma^*)$ molecular orbital, thus raising the energy of the latter.[81−83] Addition of excess py (547 $\mu$M) to **1** (22 $\mu$M) in $H_2O$ does not result in spectral shifts in the near-UV−vis regions. This result is consistent with the assignment of these low-energy transitions as $Rh_2 \rightarrow$ np MLCT, which are not expected to be affected greatly by the presence of axial ligands.

The reduction potentials of **1**−**3** are listed in Table 3. The first reduction is dependent on the identity of the aromatic ligand. Complexes **2** and **3**, with one and two coordinated pynp ligands, respectively, exhibit $E_{1/2} \sim -0.64$ V vs SCE. In contrast, complex **1** is more difficult to reduce by ∼0.17 V, with the first reduction observed at −0.82 V vs SCE. The free pynp ligand is easier to reduce than the np ligand, with $E_{1/2}$ values of −1.68 and −1.88 V versus SCE ($CH_3CN$, 0.1 M $Bu_4NPF_6$), respectively. The difference in the reduction potentials of the free ligands, 0.20 V, is comparable to that between **1** and complexes **2** and **3**. The values of the first reduction waves of complexes **1**−**3** are similar to those reported for other dirhodium complexes possessing aromatic ligands, such as *cis*-$[Rh_2(\mu\text{-}O_2CCH_3)_2(bpy)_2]^{2+}$ ($E_{1/2}$ = −0.93 V vs SCE in $CH_3CN$) and *cis*-$[Rh_2(\mu\text{-}O_2CCH_3)_2(phen)_2]^{2+}$ ($E_{1/2}$ = −0.87 V vs SCE in $CH_3CN$).[77] The oxidation potentials, $E_{1/2}$ ($[Rh_2]^{3+/2+}$), are quasi-reversible or irreversible with approximate values of +1.3 V vs SCE for **1** and +1.50 V (in each case) versus SCE for **2** and **3**. These values are similar to those previously reported for the metal-centered oxidation of related dirhodium complexes, such as $Rh_2(\mu\text{-}O_2CCH_3)_4$ with $E_{1/2}$ =+1.17 V vs SCE in $CH_3CN$.[84] These results point at the oxidation of **1**−**3** as being centered on the dirhodium core.

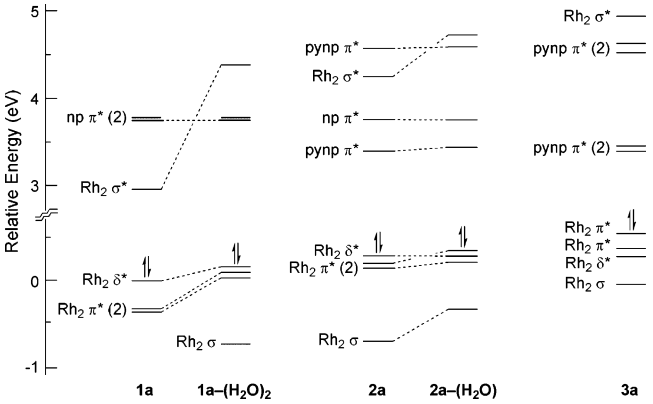


**Figure 3.** MO diagrams of (a) **1a** and **1a**−$(H_2O)_2$, (b) **2a** and **2a**−$(H_2O)$, and (c) **3a**. For reference, the $Rh_2(\delta^*)$ MO in **1a** was set to 0 eV (see text).

**Electronic Structure Calculations.** Electronic structure calculations were conducted in order to aid in the assignments of the absorption spectra and electrochemistry of complexes **1**−**3**, and comparisons were made regarding the structural and electronic changes that take place upon axial coordination of solvent and as the bridging ligands are varied. As shown in Figure 3, the electronic structures of the model complexes *cis*-$[Rh_2(\mu\text{-}O_2CH)_2(np)_2]^{2+}$(**1a**) and *cis*-$[Rh_2(\mu\text{-}O_2CH)_2(pynp)(np)]^{2+}$(**2a**) are sensitive to the nature of the coordinating solvent in the axial position as previously reported for other dirhodium complexes.[65]

In aqueous solution, water molecules coordinate to the open axial sites of **1a** and **2a** generating **1a**−$(H_2O)_2$ and **2a**−$H_2O$, respectively (Figure 3). Interaction of the symmetric and antisymmetric linear combinations of the axial water molecules with metal-centered MOs in **1a** results in the destabilization of the $Rh_2(\sigma)$ and $Rh_2(\sigma^*)$ orbitals in **1a**−$(H_2O)_2$ (Figure 3). As shown in Figure 3, these axial interactions change the identity of the LUMO from $Rh_2(\sigma^*)$ in **1a** to np($\pi^*$) in **1a**−$(H_2O)_2$. The electronic structure calculations with NCH axial ligands as models for acetonitrile molecules also result in np($\pi^*$) LUMO in **1a**−$(NCH)_2$. These results are in agreement with the observation of ligand-centered reduction of **1** in $CH_3CN$. DFT calculations on **2a**, **2a**−$(H_2O)$, and *cis*-$[Rh_2(\mu\text{-}O_2CH)_2(pynp)_2]^{2+}$ (**3a**) also result in ligand-centered LUMO in agreement with the electrochemical reduction discussed above (Figure 3). It should be noted that the calculations also predict that the reduction potentials of **2** and **3** should be similar in a coordinating solvent whereas **1** should be more difficult to reduce (Figure 3). Selected molecular orbitals of **1a**−$(H_2O)_2$, **2a**−$(H_2O)$, and **3a** are shown in the Supporting Information.

The changes to the orbital energies of **1a**−$(H_2O)_2$ upon substitution of one and two np ligand(s) for pynp to generate **2a**−$H_2O$ and **3a**, respectively, are also shown in Figure 3. In order to make a semiquantitative comparison among the complexes, the energy of the $Rh_2(\delta^*)$ MO of **1a** was set to 0.0 eV. In addition, the lowest energy np($\pi^*$) orbitals of **1a**,

(77) Crawford, C. A.; Matonic, J. H.; Huffman, J. C.; Folting, K.; Dunbar, K. R.; Cristou, G. *Inorg. Chem.* **1997**, *36*, 2361.
(78) Martin, D. S., Jr.; Webb, T. R.; Robbins, G. A.; Fanwick, P. E. *Inorg. Chem.* **1979**, *18*, 475.
(79) Dubicki, L.; Martin, R. L. *Inorg. Chem.* **1970**, *9*, 673.
(80) (a) Cotton, F. A.; Felthouse, T. R. *Inorg. Chem.* **1981**, *20*, 584. (b) Clark, R. J. H.; Hempleman, A. J. *Inorg. Chem.* **1989**, *28*, 746.
(81) Norman, J. G.; Kolari, H. J. *J. Am. Chem. Soc.* **1978**, *100*, 791.
(82) Bursten, B. E.; Cotton, F. A. *Inorg. Chem.* **1981**, *20*, 3042.
(83) (a) Sowa, T.; Kawamura, T.; Shida, T.; Yonezawa, T. *Inorg. Chem.* **1983**, *22*, 56. (b) Nakatsuji, H.; Ushio, J.; Kanda, K.; Onishi, Y.; Kawamura, T.; Yonezawa, T. *Chem. Phys. Lett.* **1981**, *79*, 299.
(84) Chavan, M. Y.; Zhu, T. P.; Lin, X. Q.; Ahsan, M. Q.; Bear, J. L.; Kadish, K. M. *Inorg. Chem.* **1984**, *23*, 4538.

**1a**−$(H_2O)_2$, **2a**, and **2a**−$(H_2O)$ were matched in energy in Figure 3, since this orbital is not expected to be affected by axial substitution. Similarly, the lowest energy pynp($\pi^*$) in **2a**−$(H_2O)$ and **3a** were set to the same energy. As expected, substitution of $H_2O$ molecules in the axial position for the stronger pyridine portion of the pynp ligand results in an increase in the energy of both the $Rh_2(\sigma)$ and $Rh_2(\sigma^*)$ MOs (Figure 3).

Time-dependent DFT (TDDFT) calculations can be used to predict observed transition energies and can be used to elucidate their parentage. As discussed above, the peaks observed in the UV region can be ascribed to $\pi\pi^*$ transitions centered on the aromatic ligands, while the two lowest energy transitions are assigned as $Rh_2 \rightarrow$ np/pynp MLCT. In general, the MLCT peaks red-shift across the series **1**−**3** (Table 3). TDDFT calculations on **1a**−$(H_2O)_2$ predict a strong np-centered transition at 259 nm and four weaker ones in the 261−275 nm range (Supporting Information). Two low-energy vertical $Rh_2(\pi^*) \rightarrow$ np($\pi^*$) MLCT transitions are calculated at 402 and 410 nm. The latter has the largest oscillator strength (Supporting Information) and may be correlated to the peak observed at 393 nm in the complex (Table 3). In **3a**, MLCT transitions from $Rh_2(\delta^*)$ and $Rh_2(\sigma^*)$ to pynp($\pi^*$) are calculated at 466 and 489 nm, respectively (Supporting Information), which may be correlated with the absorption peak with maximum at 465 nm in **3**. Additional MLCT transitions of **3a** are predicted at 315, 320, and 331 nm; however, a very strong pynp-centered transition of significantly greater intensity is calculated at 326 nm (Supporting Information). The latter may be associated with the observed peak with maximum at 356 nm in **3**. A transition at 340 nm, calculated to exhibit both MLCT and LC character in **3a**, may also contribute to the peak observed at 356 nm in **3**. Owing to the presence of both np and pynp ligands in the tris-heteroleptic complex, there is a greater number of calculated transitions for **2a**−$(H_2O)$ in the same energy range. Two low-lying MLCT transitions of similar intensity from $Rh_2(\pi^*)$ to pynp($\pi^*$) and to np($\pi^*$) are calculated at 471 and 423 nm, respectively (Supporting Information). These are at significantly lower energy than the observed MLCT peak in **2** with maximum at 398 nm (Table 3). A fairly strong pynp $\pi\pi^*$ transition is calculated at 342 nm for **2a**−$(H_2O)$ with several additional peaks with MLCT character between 318 and 335 nm. As a result of a large number of calculated peaks, a correlation with the experiment in solution for this complex is not possible. However, the calculated transitions lie in the region where the peaks are observed. As previously assigned, the calculations show that the lowest energy transition in each of these complexes is MLCT in character.

As discussed above, the metal-centered $Rh_2(\pi^*) \rightarrow Rh_2(\sigma^*)$ transition of the parent complex $Rh_2(O_2CCH_3)_4$ is known to shift to higher energy as a function of the axial ligands.[85,86] Although this weak transition is not observed experimentally in complexes **2** and **3** owing to the overlapping high-intensity MLCT peaks, its position can be calculated. As expected, the calculated energy of $Rh_2(\pi^*) \rightarrow Rh_2(\sigma^*)$ transition shifts as the number of pynp ligands with strong axial coordination is increased in the series **1a**−$(H_2O)_2$, **2a**−$(H_2O)$, and **3a** with predicted maxima at 521 nm ($f = 0.0011$), 474 nm ($f = 0.0022$), and 455 nm ($f = 0.0008$), respectively. The calculated maximum of the metal-centered transition for **1a**−$(H_2O)_2$ agrees well with the observed shoulder for **1** in water at ~519 nm.

(85) Boyar, E. B.; Robinson, S. D. *Coord. Chem. Rev.* **1983**, *50*, 109.
(86) Felthouse, T. R. *Prog. Inorg. Chem.* **1982**, *29*, 73.

**Table 4.** DNA Binding Constants, $\Delta T_m$ Values, and $C_{inh}{}^{50}$ of **1**−**3**

| complex | $K_b/M^{-1}$ | $\Delta T_m/{}^oC$[a] | $C_{inh}{}^{50}/\mu M$[b] |
|---|---|---|---|
| **1** | $5.6 \times 10^5$ | 10.3 | 3.4 |
| **2** | $3.4 \times 10^5$ | 7.0 | 54 |
| **3** | $3.3 \times 10^3$ | 4.2 | >600 |

[a] $T_m = 61(1)$ °C was measured for DNA alone. [b] The value measured for cisplatin under the same experimental conditions was 4.1 $\mu$M.

**DNA Binding.** The binding constants of **1**−**3** to DNA, $K_b$, determined from fits of the changes in the absorption of each complex as a function of nucleic acid concentration are listed in Table 4. The values of $K_b$ vary with the availability of the axial position. For complex **1**, with both axial positions available for coordination with Lewis bases, $K_b = 5.6 \times 10^5\ M^{-1}$ ($s = 1.1$) was measured, while $K_b = 3.4 \times 10^5\ M^{-1}$ ($s = 0.9$) was calculated for **2**. The value of $K_b$ measured for **3** ($3.3 \times 10^3\ M^{-1}$ ($s = 2.0$)), which has the two axial positions blocked by the pynp ligand, is approximately 2 orders of magnitude smaller than the DNA binding constants of **1** and **2**. The magnitude of $K_b$ obtained for **3** is consistent with electrostatic interactions between the complex and DNA, where similar values have been reported in the literature for $[Ru(tpy)(bpy)OH]^+$ (tpy = 2,2′:6′,2″-terpyridine, $K_b = 1.3 \times 10^4\ M^{-1}$), $[Ru(tpy)(bpy)(OH_2)]^{2+}$ ($K_b = 6.6 \times 10^2\ M^{-1}$), and $[Ru(bpy)_3]^{2+}$ ($K_b = 6.8 \times 10^2\ M^{-1}$), which bind DNA through electrostatic interactions.[87] For comparison, the DNA binding constant for the partial intercalator $[Ru(phen)_3]^{2+}$ was reported[87b] to be $4.8 \times 10^3\ M^{-1}$ while a $K_b$ value of $1.7 \times 10^5\ M^{-1}$ has been reported for the intercalator ethidium bromide.[88] Since complexes **1**−**3** have the same overall charge, the differences in measured $K_b$ values are not due to electrostatic interactions. Previous reports have shown that dirhodium compounds can interact with DNA forming a variety of interstrand cross-link adducts.[89] Therefore, it is possible that there is a covalent interaction between the open axial position of the compound and the DNA such that the decrease in the value of the binding constant from **1** to **2** is related to the difference in the number of open axial positions.

The shift in the melting temperature of 100 $\mu$M DNA, $\Delta T_m$, in the presence of each complex (20 $\mu$M) was measured relative to that of DNA alone, for which $T_m = 61(1)$ °C (1 mM phosphate buffer, 2 mM NaCl, pH 7.2). The largest shift, $\Delta T_m = +10(2)$ °C, was observed for compound **1** followed

(87) (a) Kalsbeck, W. A.; Thorp, H. H. *Inorg. Chem.* **1994**, *33*, 3427−3429. (b) Kalsbeck, W. A.; Thorp, H. H. *J. Am. Chem. Soc.* **1993**, *115*, 7146.
(88) (a) Tang, T.-C.; Huang, H.-J. *Electroanalysis* **1999**, *11*, 1185. (b) Paoletti, C.; Le Pecq, J. B.; Lehman, I. R. *J. Mol. Biol.* **1971**, *55*, 75.
(89) Dunham, S. U.; Chifotides, H. T.; Mikulski, S.; Burr, A. E.; Dunbar, K. R. *Biochemistry* **2005**, *44*, 996.

by **2** with $\Delta T_m = +7(2)$ °C. Only a modest shift in the DNA melting temperature was measured for **3**, $\Delta T_m = +4(2)$ °C. Intercalating complexes possessing a phi (phi = 9,10-phenanthrenequinone diimine) ligand in their coordination sphere, such as $[Rh(phen)_2phi]^{3+}$ and $[Ru(phen)_2phi]^{2+}$, were previously shown to raise the melting temperature of the duplex by 7 and 11 °C, respectively.[73] Similar stabilization of the DNA double helix has been reported for other intercalators, such as $[Ru(bpy)_2(DAP)]^{2+}$ (DAP = 1,12-diazaperylene) and ethidium bromide.[72] Therefore, it is possible that the shift in $T_m$ observed for **1** is due to DNA intercalation by the complex. Intercalation of molecules between DNA bases is known to increase the viscosity of the solution owing to unwinding and elongation of the double helix.[90] Experiments using 1 mM herring sperm DNA in the presence of up to 300 $\mu$M of **1** did not result in an increase of the relative viscosity of the solution (Supporting Information). Since relative viscosity measurements are the most reliable means to determine intercalation,[90] these results indicate that the greater DNA binding constant and $\Delta T_m$ value measured for **1** is not due to intercalation.

A possible explanation for these observations is the presence of one and two axial sites available for coordination in **1** and **2**, respectively; whereas the two rhodium centers in **3** are coordinatively saturated, since the pynp ligands block both axial sites in the complex. It is well known that cations, such as $Na^+$ and $Mg^{2+}$, stabilize the duplex DNA structure by charge screening through interaction with the anionic phosphate groups in the phosphodiester backbone.[91−93] It has been previously shown that divalent alkaline-earth ions are able to stabilize the duplex structure to a significantly greater extent than monovalent cations.[91−93] For example, the melting temperature of a duplex composed of the sequence d(GCCAGTTAA) and its complementary strand was reported to increase from 32.0 °C in the presence of 100 mM NaCl (10 mM $Na_2HPO_4$, 1 mM $Na_2EDTA$, pH = 7.0) to 39.0 °C in 100 mM $MgCl_2$ (10 mM sodium cacodylate, pH = 7.0).[94] A similar shift in $T_m$ was measured for the same duplex in the presence of 10 mM $MgCl_2$ ($T_m$ = 36.0 °C) and in mixtures of 100 mM NaCl with 10 mM $MgCl_2$ ($T_m$ = 35.1 °C) and with 100 mM $MgCl_2$ ($T_m$ = 38.5 °C).[94] These results show the greater activity of divalent ions in duplex stablization compared to monovalent cations. In contrast to the increase in the DNA melting temperature typically observed for divalent alkaline earth ions, transition metal cations, such as $Co^{2+}$, $Ni^{2+}$, and $Cd^{2+}$, result in destabilization of the duplex.[95] It is believed that cations that interact with the phosphate backbone stabilize the duplex DNA structure, and those that coordinate to the nucleobases have a destabilizing effect.[95]

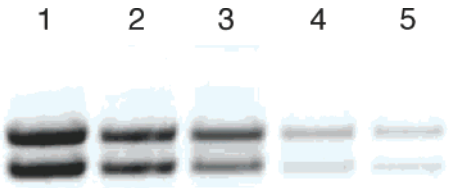


**Figure 4.** Ethidium bromide stained agarose gel showing mRNA produced in the transcription reaction in the absence (lane 1) and in the presence of 2 $\mu$M (lane 2), 4 $\mu$M (lane 3), 6 $\mu$M (lane 4), and 10 $\mu$M (lane 5) of **1**.

Similarly, non-intercalating mononuclear cationic transition metal complexes that interact with the phosphodiester backbone of duplex DNA exhibit positive $\Delta T_m$ values consistent with electrostatic screening of the negative phosphate charges.[96,97] A modest increase in DNA melting temperature, +5 °C, was previously reported for $[Ru(phen)_3]^{2+}$ and $Rh(phen)_3]^{3+}$.[73] Monofunctional cationic complexes, such as $[Pt(NH_3)_3Cl]^+$ and $[Pt(dien)Cl]^+$ (dien = diethylenetriamine), that interact through coordination to the N7 position of guanine typically shift the $T_m$ values to lower temperatures.[98,99] In these systems, however, the destabilization that results from the conformational changes that take place upon guanine coordination competes with electrostatic screening, thus, making shifts in $T_m$ highly dependent on nucleic acid sequence and salt concentration.[99]

Complexes **1** and **2** may be able to efficiently screen the charge on the DNA backbone through axial interactions with the oxygen atoms of the phosphodiester backbone of the duplex, thus resulting in $\Delta T_m$ values of +10(2) and + 7(2) °C, respectively. The blue shift in $Rh_2(\pi^*) \rightarrow Rh_2(\sigma^*)$ transition observed in the absorption spectrum of $Rh_2(O_2CCH_3)_4$ upon addition of DNA is indicative of axial coordination;[42] however, owing to its overall zero charge, no shift in the DNA melting temperature was observed.[100] The lower shift in $T_m$ of **3**, +4 °C, may be due to the inability of the complex to interact effectively with the DNA backbone, thus reducing charge screening.

**Transcription Inhibition.** The inhibition of transcription by each metal complex was determined by recording the imaged mRNA produced during the transcription reaction as a function of complex concentration while keeping the concentrations of all other components constant. A typical imaged gel is shown in Figure 4 for **1** and those for **3** are shown in the Supporting Information. For complex **1** (Figure 4), the mRNA produced decreases relative to the control lane (no metal complex, Lane 1) as the complex concentration is increased from 1.5 to 7.5 $\mu$M (Lanes 2−5).

(90) Suh, D.; Oh, Y.-K.; Chaires, J. B. *Process Biochem.* **2001**, *37*, 521.
(91) Subirana, J. A.; Soler-López *Annu. Rev. Biophys. Biomol. Struct.* **2003**, *32*, 27.
(92) Williams, L. D.; Maher, L. J., III. *Annu. Rev. Biophys. Biomol. Struct.* **2000**, *29*, 497.
(93) Hud, N. V.; Polak, M. *Curr. Opin. Struct. Biol.* **2001**, *11*, 293.
(94) Nakano, S.; Fujimoto, M.; Hara, H.; Sugimoto, N. *Nucleic Acids Res.* **1999**, *27*, 2957.
(95) Duguid, J. G.; Bloomfield, V. A.; Benevides, J. M.; Thomas, G., Jr. *Biophys. J.* **1995**, *69*, 2623.
(96) Tselepi-Kalouli, E.; Katsaros, N. *J. Inorg. Biochem.* **1989**, *37*, 271.
(97) Karpel, R. L.; Bertelsen, A. H.; Fresco, J. R. *Biochemistry* **1980**, *19*, 504.
(98) van Garderen, C. J.; van den Elst, H.; van Boom, J. H.; Reedijk, J. *J. Am. Chem. Soc.* **1989**, *111*, 4123.
(99) (a) Brabec, V.; Reedijk, J.; Leng, M. *Biochemistry* **1992**, *31*, 12397. (b) Zaludová, R.; Kleinwächter, V.; Brabec, V. *Biophys. Chem.* **1996**, *60*, 135.
(100) Tselepi-Kalouli, E.; Katsaros, N. *J. Inorg. Biochem.* **1990**, *40*, 95.
(101) *CRC Handbook of Chemistry and Physics*, 81st ed.; Lide, D. R., Ed.; CRC Press: New York, 2000, pp 8-46−8-47.
(102) Kashik, T. V.; Rassolova, G. V.; Ponomareva, S. M.; Medvedeva, E. N.; Yushmanova, T. I.; Lopyrer, V. A. *Izv. Akad. Nauk SSSR, Ser. Khim.* **1982**, *10*, 2230.

In contrast, no decrease in the mRNA transcribed is observed upon addition of up to 300 $\mu$M of **3** (Figure S3). The concentration of each complex required to inhibit 50% of the transcription, $C_{inh}^{50}$, was determined from interpolation of plots of percent inhibition as a function of increasing complex concentration. The values of $C_{inh}^{50}$ for **1** and **2** are 3.4 and 54 $\mu$M, respectively, while that for **3** could not be measured but can be estimated to be $>600$ $\mu$M (Table 3).

A strong correlation between the DNA melting temperature of mononuclear Ru(II) and Rh(III) complexes with transcription inhibition has been previously reported.[73] It is believed that the stabilization of the DNA duplex structure suppresses bubble formation thus reducing the amount of transcribed RNA. In the present work, this trend is also observed with an increase in transcription inhibition with greater duplex stabilization. Additional studies are currently underway to gain further understanding of whether the interactions of the complex with DNA or with the enzyme result in the reduced production of RNA.

## Conclusions

Dirhodium(II,II) complexes that possess one or two accessible axial coordination sites, *cis*-$[Rh_2(OAc)_2(np)_2]^{2+}$ (**1**) and *cis*-$[Rh_2(OAc)_2(np)(pynp)]^{2+}$ (**2**), respectively, were compared to a compound in which the axial sites are blocked, *cis*-$[Rh_2(OAc)_2(pynp)_2]^{2+}$ (**3**). In the latter, the bridging pynp ligand blocks both the axial coordination sites in the complex. The electronic and electrochemical properties of the complexes were investigated, and TDDFT calculations were used to aid in the assignments. The ability of the complexes to stabilize duplex DNA and to inhibit transcription *in vitro* shows a profound effect on the availability of an axial coordination site on reactivity toward biomolecules.

**Acknowledgment.** K.R.D. thanks Johnson-Matthey for a generous gift of $Rh_2(\mu\text{-}O_2CCH_3)_4$. C.T. thanks the National Science Foundation (CHE 0503666) and the Ohio Supercomputing Center. K.R.D. thanks the State of Texas for an ARP Grant (010366-0277-1999) and the Welch Foundation (A1449) for financial support. D.A.L. thanks The Ohio State University for a Presidential Fellowship.

**Supporting Information Available:** Selected molecular orbitals, TDDFT energies and assignments, relative viscosity experiments, additional transcription inhibition gels in the presence of **3**, DNA binding titrations, and crystallographic parameters. This material is available free of charge via the Internet at http://pubs.acs.org.

IC700708G